Research Article

Pulmonary Circulation

Improvement of lung ischemia–reperfusion injury by inhibition of microRNA-155 via reductions in neuroinflammation and oxidative stress of vagal afferent nerve

Yan Zhou*, Lianjie Zhang*, Jingjing Guan and Xin Yin

Department of Thoracic Surgery, The First Hospital of Jilin University, Changchun, China

Abstract

Lung ischemia–reperfusion injury (LIRI) is a common clinical concern. As the injury occurs, the pulmonary afferent nerves play a key role in regulating respiratory functions under pathophysiological conditions. The present study was to examine the effects of inhibiting microRNA-155 on the levels of proinflammatory cytokines and products of oxidative stress in the pulmonary vagal afferent nerves and the commissural nucleus of the solitary tract (cNTS) after LIRI. A rat model of LIRI was used. ELISA method was employed to examine proinflammatory cytokines, namely, IL-1β, IL-6 and TNF-α; and key biomarkers of oxidative stress, 8-isoprostaglandin F2α (8-iso PGF2α) and 8-hydroxy-2′-deoxyguanosine (8-OHdG). In results, in the process of LIRI, the levels of microRNA-155 were amplified in the vagal afferent nerves and cNTS, and this was accompanied with increases of IL-1β, IL-6 and TNF-α; and 8-iso PGF2α and 8-OHdG. Application of microRNA-155 inhibitor, but not its scramble, attenuated the elevation of proinflammatory cytokines and amplification of 8-iso PGF2α and 8-OHdG in those nerve tissues. In conclusion, we observed the abnormalities in the pulmonary afferent pathways at the levels of the peripheral nerves and brainstem, which is likely to affect respiratory functions as LIRI occurs. Our data suggest that blocking microRNA-155 signal pathways plays a beneficial role in regulating LIRI via inhibiting responses of neuroinflammation and oxidative stress signal pathways to LIRI.

Keywords

miRNA-155, neuroinflammation, oxidative stress, lung ischemia, brainstem, vagal nerves

Date received: 12 February 2020; accepted: 25 March 2020

Pulmonary Circulation 2020; 10(2) 1–8

DOI: 10.1177/2045894020922125

Introduction

Lung ischemia–reperfusion injury (LIRI) is a common and severe postoperative complication that often occurs after lung transplantation, cardiopulmonary bypass, cardiopulmonary resuscitation, pulmonary embolism, and sepsis.[1,2] Although surgical technology is developed, an inevitable surge in LIRI remains in clinics due to its wide application. The underlying mechanisms leading to LIRI are mainly due to inflammation, oxidative stress, cellular apoptosis and intracellular calcium overload.[3] Nonetheless, it is noteworthy to determine molecular mediators and their signal pathways involved in pathophysiological process of LIRI.

Pulmonary sensory nerves play an essential role in regulating respiratory functions to maintain homeostasis.[4] A large subset of afferents in the vagus nerves respond to inflammatory mediators and oxidative stress and noxious stimuli.[4] Under pathophysiological conditions, stimulation of a variety of receptors in sensory nerves has been reported to mediate neurogenic inflammatory and oxidative stress responses.[5–8] In the process of ischemic stress response,

*These authors have equal contribution to this work as co-first authors.

Corresponding authors:

Jingjing Guan, Department of Thoracic Surgery, The First Hospital of Jilin University, 71 Xinmin Street, Changchun 130021, China.

Email: guanj@163.com

Xin Yin, Department of Thoracic Surgery, The First Hospital of Jilin University, 71 Xinmin Street, Changchun 130021, China.

Email: xinyin@163.com

the levels of proinflammatory cytokines (PICs) are increased and a number of receptors associated with PIC stimulation are upregulated in nodose ganglions (NG).[9] Note that the NG neurons primarily supply sensory pulmonary vagal nerves and send sensory signals to the central nervous system.

Sensory input from nerve endings in the lungs is sent to vagal afferent neurons in the lower nodose and superior jugular ganglions. The nodose ganglion is derived from epibranchial placodes and the jugular ganglions originate from the neural crest cells, which define the phenotypes of the vagal fibers.[10] Primary respiratory vagal reflexes modifying the pattern of breathing are evoked via lung inflation and activation of chemoreceptors by chemical substances affecting vagal afferents.[4] The central endings of vagal afferent neurons innervating the airways terminate in the medulla oblongata (such as the commissural nucleus of the solitary tract (cNTS)) and release a variety of neurotransmitters and neuromodulators,[4] which thereby affects vagal motor neurons in the brainstem.

MicroRNAs (miRNAs) are small noncoding endogenous RNA molecules that can alter their target mRNA through binding in the message 3′-UTR.[11] MiRNAs have been shown to have important contributions to multiple pathophysiological processes: cellular death and survival, cellular response to stress, stem cell division, and pluripotency.[12] MiRNAs also play a role in regulating disease processes including cancer, cardiovascular and neurological diseases.[13–15] As a result of their small size, relative ease of delivery, and sequence specificity in recognizing their targets, miRNAs have been considered as promising therapeutic targets with respect to drug development.[16]

Among various miRNAs, miRNA-155 (miR-155) plays a role in various physiological and pathological processes.[17–20] MiR-155 is involved in chronic immune response by amplifying the proliferative response of T cells via the downregulation of lymphocyte-associated antigens.[21] In autoimmune disorders, a higher expression of miR-155 is observed in patients' tissues and synovial fibroblasts.[19] In multiple sclerosis, upregulation of miR-155 has been observed in peripheral nerve and CNS-resident myeloid cells, blood monocytes in the circulation and stimulated microglia.[22] Also, a prior study has suggested that miR-155 is involved in inflammation and upregulation of miR-155 in chronic inflammation in human.[20]

Thus, we hypothesized that LIRI upregulates miR-155 in the NG and cNTS, which amplifies the levels of cytokines (such as IL-1β, IL-6 and TNF-α) and oxidative stress products (namely, 8-isoprostaglandin F2α (8-iso PGF2α) and 8-hydroxy-2′-deoxyguanosine (8-OHdG)) in these peripheral and central nervous regions of rats. We further hypothesized that blocking miR-155 signal pathway decreases the upregulation of PICs and oxidative stress products in signal pathways of the pulmonary afferent inputs induced by LIRI.

Methods

Animal

All animal protocols were in accordance with the guidelines of the International Association for the Study of Pain and approved by the Animal Care and Use Committee of Jilin University. Male Sprague-Dawley (200–250 g) were housed in individual cages with free access to food and water and were kept in a temperature-controlled room (25°C) on a 12/12-h light/dark cycle.

Lateral ventricle cannulation

The rats were anesthetized with sodium pentobarbital (60 mg/kg body weight, i.p.) and immobilized in a stereotaxic apparatus (David Kopf, USA). After making a midline incision, the skull was exposed and one burr hole was drilled. Following this, animals were cannulated with an L-shaped stainless steel cannula aimed at the lateral ventricle according to the coordinates: 3.7 mm posterior to the bregma, 4.1 mm lateral to the midline, and 3.5 mm under the dura. The guide cannula was fixed to the skull using dental zinc cement. Then, the cannula was connected to an osmotic minipump (Alzet pump brain infusion kit, DURECT Inc., Cupertino, CA) with polycarbonate tubing as described previously.[23] The pumps were placed subcutaneously between the scapulae and the pumps were loaded with miR-155 inhibitor (5′AAU UAC GAU UAG CAC UAU CCC CA-3′) and its corresponding scramble for negative controls (5 μg in artificial cerebrospinal fluid, Biomics Biotech, Nantong, China), respectively. The inhibitor and scramble were delivered for a period of 24 h at a rate at 0.25 μl per hour. This intervention allowed us to give continuously drugs via intracerebroventricular (ICV) infusion.

A model of lung ischemia–reperfusion injury

The rats were initially anesthetized using pentobarbital sodium (60 mg/kg, i.p.) and then anesthesia was maintained by continuous infusion of pentobarbital (0.05 mg/kg/min). An endotracheal tube was inserted and the rats were ventilated using a rat ventilator (Harvard Apparatus, Boston, MA). The ventilating parameters were set with an inspiratory oxygen fraction (FiO2) of 40% at a rate of 50–60 breaths/min and a tidal volume of 6–8 mL/kg.

Catheters were inserted into the femoral artery and vein for monitoring arterial blood pressure and administration of fluids (saline, 1 mL/h) and drugs (vecuronium bromide, 0.1 mg/kg/h; heparin, 250 U/kg), respectively. A left anterolateral thoracotomy was performed in the fifth intercostal space, and the pleura were exposed to allow the left hilum of the lung to be isolated. After stabilizing for 15 min, the tidal volume was decreased to 5–7 mL/kg, and the rate was increased to 70–75 breaths/min. Lung ischemia was induced by clamping the left pulmonary hilum, including the left main bronchus, artery and vein, for 1 h, followed by

reperfusion induced by removing the clamp and ventilating the left lung for 6 h as reported previously.[23] The sham control group (''sham control'') underwent the left thoracotomy without clamping hilus and was ventilated for 7 h.

The thoracic incision was protected from evaporative losses using a covering of wet absorbent gauze. The body heat of the rats was maintained using a heating lamp at a rectal temperature within the normal range (36–37°C). Arterial blood (0.3 mL) was collected from each rat before induction of ischemia and 30 min and 2.5 and 5 h after reperfusion, and then blood gas analyses were performed (ABL 800; Radiometer, Copenhagen, Denmark). Arterial partial pressure of oxygen (PaO_2) and arterial partial pressure of carbon dioxide ($PaCO_2$) were also recorded. The arterial pressure, heart rate, and temperature of each rat were also monitored continuously throughout the study. At the end of the experiment, the rats were euthanized with pentobarbital sodium (120 mg/ kg, i.p.), and under an anatomical microscope, the NG and brainstem were taken out to determine the levels of PICs, and 8-iso PGF2α and 8-OHdG.

Real-time PCR

For measurement of miR-155 levels, the NG and brain were taken out just after the LIRI and 1, 3 and 6 h after LIRI. The tissues were processed for the extraction of total RNA (RNeasy Mini Kit; Qiagen, CA). The TaqmanW Universal PCR Master Mix was used to conduct RT-PCR. For the mRNA amplification, this mix has AmpliTaq GoldW DNA Polymerase, AmpEraseW UNG, ROX passive reference, buffer and dNTPs, and gene-specific primers. 18 s rRNA was also used as an endogenous control to correct for variations in the samples. RT-PCR was conducted in duplicate in 96-well plates containing 2 μL of cDNA. The thermal conditions of the cycles were 50°C for 2 min, 60°C for 30 min, and 95°C for 5 min and this procedure was followed by 40 cycles at 94°C for 20 s and 62°C for 60 s. The data were obtained in the ABI PRISM SDS 7000 thermal cycler. The $2^{-\Delta\Delta Ct}$ comparative method was used to obtain relative quantification of target gene expression and the threshold cycle value was determined by the point at which there was a statistically significant amplification in fluorescence.

ELISA measurement

The NG and cNTS tissues of the rats were obtained under an anatomical microscope. All the tissues from individual rats were sampled for the analysis. Total protein was then extracted by homogenizing the sample in ice-cold immunoprecipitation assay buffer with protease inhibitor cocktail kit. The lysates were centrifuged and the supernatants were collected for measurements of protein concentrations using a bicinchoninic acid assay reagent kit. The levels of 8-iso PGF2α and 8-OHdG were examined using an ELISA assay kits (obtained from Promega Co. US and Abcam Co.US) according to the provided description. Briefly, polystyrene 96-well microtitel immunoplates were coated with affinity-purified rabbit primary antibodies. Parallel wells were coated with purified rabbit IgG for the evaluation of nonspecific signal. After overnight incubation, plates were washed. Then, the diluted samples and 8-iso PGF2α/8-OHdG standard solutions (100 pg/ml–100 ng/ml) were distributed in each plate. The plates were washed and incubated with anti-8-iso PGF2α/8-OHdG galactosidase. Then, the plates were washed and incubated with substrate solution. After incubation, the optical density was measured using an ELISA reader (575 nm of wavelength). In the similar way, the levels of IL-1β, IL-6 and TNF-α were also determined using an ELISA assay kits (Wuhan Fine Biotech Co, China).

Statistical analysis

All data were analyzed using one-way repeated-measures analysis of variance. Values were presented as means ± standard error of mean. For all analyses, differences were considered significant at $P < 0.05$. All statistical analyses were performed by using SPSS for Windows version 13.0 (SPSS Inc.).

Results

Blood gas and arterial blood pressure

The arterial-alveolar oxygen pressure gradient ($A\text{-}aDO_2$) was calculated using the following formula: $A\text{-}aDO_2$ = fraction inspired $O_2 \times (Patm\text{-}PH_2O) - (PaCO_2/RQ) - PaO_2$, where Patm = 760 mmHg, PH_2O = 47 mm Hg, and RQ = 0.8. In sham rats ($n = 12$), no significant differences in PaO_2 and $A\text{-}aDO_2$ were observed over baseline at any time point (Fig 1). Figure 1 also shows that in LIRI group ($n = 28$), PaO_2 decreased by 24% (1 h post-reperfusion) and by 21% (6 h post-reperfusion) compared with baseline ($P < 0.05$ vs. baseline), whereas the $A\text{-}aDO_2$ increased by 23% (1 h post-reperfusion) and by 16% (6 h post-reperfusion) ($P < 0.05$ vs. baseline). An exacerbated blood gas exchange with declined PaO_2 and elevated $A\text{-}aDO_2$ indicated the process of LIRI in the rat model used in this study.

Arterial blood pressure and heart rate were stable throughout the whole study in sham control rats (Fig 1). Although the mean arterial pressure (MAP) appeared to slightly decrease in LIRI rats, no significance difference was seen between sham control group and LIRI group (i.e. MAP: 96 ± 7 mm Hg in sham control and 93 ± 9 mmHg in LIRI 5 h post-reperfusion; $P > 0.05$ between two groups). There was no significant difference in heart rate between the two groups at any time point (i.e. 387 ± 21 beats/min in sham control group and 381 ± 21 beats/min in LIRI group 5 h after reperfusion; $P > 0.05$ between two groups).

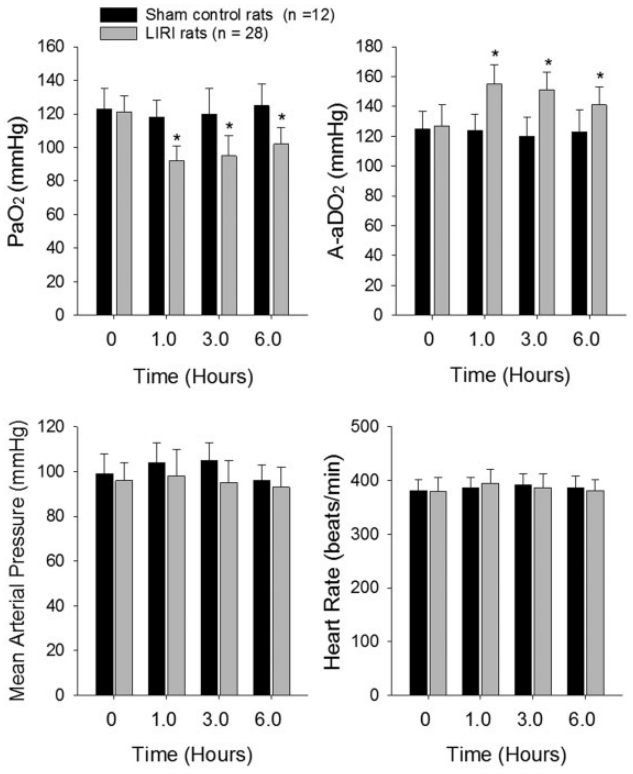

Fig. 1. Blood oxygen and carbon dioxide; and blood pressure and heart rate after lung ischemia reperfusion injury (LIRI). Top panels: Arterial partial pressure of oxygen and arterial partial pressure of carbon dioxide of rats in sham control rats and rats with LIRI. 0 h indicates baseline before ischemia; and 1.0, 3.0 and 6.0 h indicate times after reperfusion. *$P < 0.05$ vs. baseline. Bottom panels: Mean arterial pressure and heart rate of sham control rats and LIRI rats before ischemia, and 1.0–6.0 h after reperfusion. There were no differences in mean arterial pressure and heart rate for baseline and at different time points after reperfusion in sham control and LIRI groups. Note that "*n*" indicates a total number of rats in sham control group ($n = 12$) and LIRI group ($n = 28$).

Levels of miR-155 after LIRI

We examined the time course for changes of miR-155 in the afferent nerves and cNTS after LIRI. Figure 2 shows a stabilized increase in the levels of miR-155 of the NG and cNTS 6 h after the end of LIRI procedure. Based on this result, the time point of 6 h was selected to examine the effects of miR-155 inhibitor for the rest of experiments.

Levels of PICs after LIRI

In order to determine if PIC signal was involved in the effects of LIRI, in this experiment, we examined the levels of PICs in the NG and cNTS. Figure 3 shows that IL-1β, IL-6 and TNF-α were significantly increased in the NG and cNTS of LIRI rats with scramble ($P < 0.05$ vs. sham control rats; $n = 12$ in sham control rats and $n = 16$ in LIRI rats) as compared with sham control rats. Furthermore, ICV infusion of miR-155 inhibitor attenuated amplifications of PICs in the NG and cNTS evoked by LIRI. Insignificant differences in the levels of IL-1β, IL-6 and TNF-α in the NG and cNTS were observed between LIRI rats with ICV infusion of miR-155 inhibitor ($n = 15$) and sham control rats ($n = 12$; $P > 0.05$, between two group).

Level of oxidative stress products after LIRI

We further examined products of oxidative stress in the NG and cNTS of LIRI rats and sham control rats as shown in Fig 4. This figure demonstrates that 8-iso PGF2α and 8-OHdG were increased in the NG and cNTS of LIRI rats with scramble ($n = 16$) as compared with sham control rats ($n = 12$; $P < 0.05$, LIRI vs. controls). In addition, ICV infusion of miR-155 inhibitor attenuated increases of both 8-iso PGF2α and 8-OHdG in the NG and cNTS ($P < 0.05$, LIRI rats vs. LIRI rats with infusion of inhibitor/$n = 15$). Note that no significant differences in 8-iso PGF2α and 8-OHdG were observed between sham control rats and LIRI rats with miR-155 inhibitor ($P > 0.05$).

Discussion

Accumulated evidence has demonstrated critical roles played by various miRNAs in modifying pathophysiological processes with animal models and clinical ischemic disorders.[24–26] Specifically, it was reported that anti-inflammatory protein suppressor of cytokine signaling 1 (SOCS1) is one of the target genes of miR-155.[27] SOCS1 is a critical regulator of inflammation and negatively regulates the feedback of inflammation.[28] Deficiency of SOCS1 results in amplified responsiveness to inflammation in affected cells and/or in animals.[29,30] MiR-155 is also involved in regulating stroke development by promoting expression of TNF-α and IL-1β and by decreasing SOCS1.[31,32] Thus, more investigations are needed to explain the networks of miR-155 in involvement of LIRI-induced pathophysiological changes. In this report, we demonstrated that the levels of miR-155 were amplified in the vagal afferent nerves and cNTS of LIRI rats, and this was accompanied with increases of IL-1β, IL-6 and TNF-α; and 8-iso PGF2α and 8-OHdG. ICV administration of miR-155 inhibitor, but not its scramble, attenuated the elevation of PICs and amplification of 8-iso PGF2α and 8-OHdG in those nerve tissues. Our data suggest that blocking miR-155 signal pathways plays a beneficial role in regulating LIRI via inhibiting responses of neuroinflammation and oxidative stress signal pathways to LIRI.

Breathing is regulated by the nervous system to ensure appropriate tissue oxygenation. The central and peripheral sensory neurons regulate the respiratory cycle in response to changes in blood pH and gas composition.[33,34] Among these, sensory neurons of the vagus nerve are the major source of nerve fibers that innervate the lung and airways, and are important for normal breathing to maintain homeostasis. The vagus neurons contain sensory nerve that

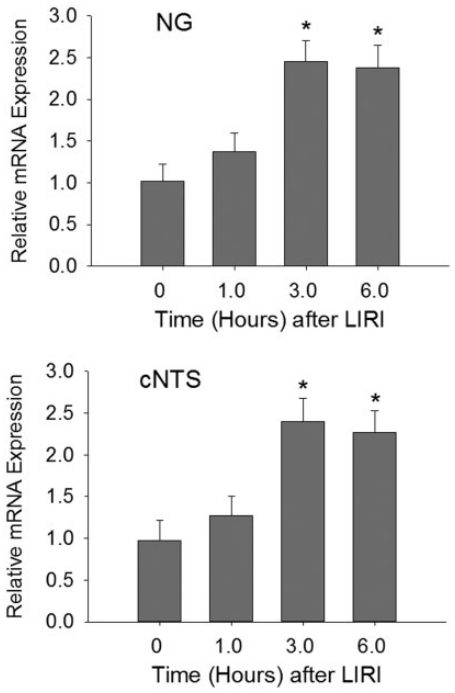

Fig. 2. The time course for the levels of miR-155 mRNA was increased in the nodose ganglion (NG) and the commissural nucleus of the solitary tract (cNTS) after the end of LIRI procedure and the increase was stabilized 6 h after the LIRI procedure and remained at a high level. *$P < 0.05$ vs. its level before LIRI (baseline). Point "0" indicates before LIRI. The number of rats = 6–10 in each group.

provides critical information needed to control respiration rate and regulates airway tone and defense.[33,35]

A large subset of sensory nerves in the vagus nerves can respond to inflammatory mediators and noxious stimuli.[4] Hypersensitivity of these afferent nerves is involved in the manifestation of various symptoms associated with airway inflammation, which include bronchoconstriction and mucus hypersecretion, accompanied by the sensation of airway irritation, and urge to cough.[4] With LIRI, cytokines produced by a broad range of cells (i.e. immune cells like macrophages, lymphocytes and mast cells) are likely presented in and affect vagal sensory nerves and change the reflex breathing response. With LIRI, oxidative stress linked to inflammation is also observed. Nevertheless, the effects of LIRI on inflammation of the vagus nerve and neurons are poorly characterized. In the current study, we showed that inhibition of miR-155 decreases LIRI-activated PICs and oxidative stress products in the pulmonary afferent pathways at the levels of the peripheral nerves and brainstem (the NG and cNTS).

Transient receptor potential ankyrin 1 (TRPA1) plays a functional role in regulating neurogenic inflammation resulting from channel activation to a variety of compounds including pungent agents, irritant chemicals, reactive oxygen, and products of oxidative stress-induced lipid peroxidation.[36–40] TRPA1 has been shown to appear in pulmonary sensory nerves and is engaged in development of inflammation-mediated responses and ischemic injury.[41–43]

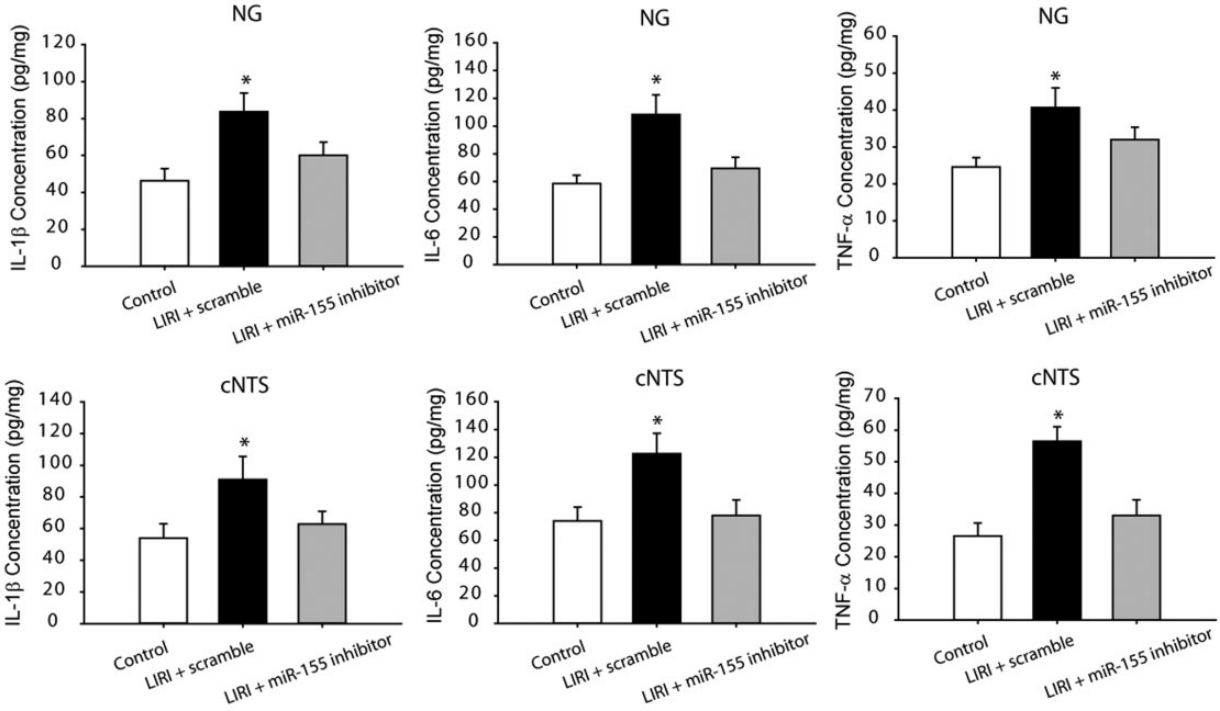

Fig. 3. The levels of IL-1β, IL-6 and TNF-α in the nodose ganglion (NG)/vagal nerve (top panels) and the commissural nucleus of the solitary tract (cNTS; bottom panels). The cytokines were significantly increased in LIRI rats with scramble as compared with control animals. MiR-155 inhibitor attenuated increases of those cytokines in the peripheral and central vagal afferent nerves of LIRI rats. *$P < 0.05$, indicated rats with LIRI with scramble ($n = 16$) vs. sham control rats ($n = 12$) and LIRI rats with miR-155 inhibitor ($n = 15$).

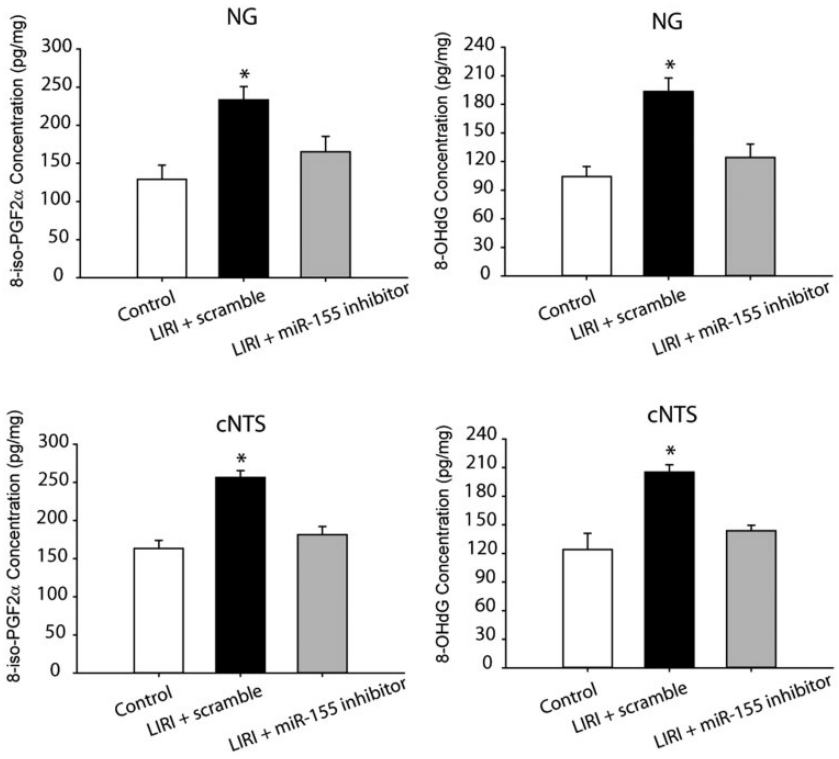

Fig. 4. Effects of LIRI on oxidative stress signal pathways. LIRI amplified the levels of oxidative products 8-iso PGF2α and 8-OHdG in the the nodose ganglion (NG) and the commissural nucleus of the solitary tract (cNTS). As miR-155 inhibitor was infused via ICV, increases of 8-iso PGF2α and 8-OHdG were attenuated. $^*P < 0.05$, LIRI rats with miR-155 scramble ($n = 16$) vs. sham control rats ($n = 12$) and LIRI rats with miR-155 inhibitor ($n = 15$).

Interestingly, recent findings suggest that roles of PICs and oxidative stress in regulating TRPA1 functions in visceral and pulmonary sensory nerves and blocking PIC signals can decrease upregulation of TRPA1 expression in sensory nerves after inflammatory responses.[6–8]

Of note, TRPA1 is also responding to reactive oxygen species (ROS).[37,44–46] ROS are considered as endogenously generated molecule mediators during oxidative stress and/or inflammation.[37,44–46] It was speculated that increases of 8-iso PGF2α and 8-OHdG induced by LIRI upregulated TRPA1 expression in the NG. Nonetheless, our current data showed that blocking miR-155 signal pathway can attenuate neuroinflammation and oxidative stress in the NG and cNTS. PICs including IL-1β, IL-6 and TNF-α have been reported to be involved in sensory vagal nerve-mediated reflex response.[47] A prior study has suggested that PICs and some receptors activated by PIC were increased in the NG of rats with stress insult.[9] Taken together, data of our current study suggest the role of miR-155 in regulating vagal afferent inputs during the process of LIRI via activation of products of PICs and oxidative stress, by which respiratory functions are likely to be adjusted to maintain homeostasis. Our current data further suggest that inhibition of miR-155 signal plays a beneficial role in alleviating LIRI-amplified PICs and oxidative stress products in the NG.

In involvement of respiratory vagal reflexes, the cNTS can receive afferent inputs from the central endings of vagal sensory neurons innervating the airways and modify the pattern of breathing and thereby affect vagal motor neurons in the brainstem.[4] In a previous study, the effects of LIRI on antioxidant response and oxidative stress signal pathways in the cNTS were observed and it was found that the expression of Nrf2-ARE signal and SOD expression was downregulated in the cNTS of LIRI rats. In addition, LIRI upregulated the expression of NOX4 in the cNTS. Thus, it is well reasoned that products of oxidative stress 8-iso PGF2α and 8-OHdG were increased in the cNTS by LIRI.

In conclusions, LIRI leads to increases in neuroinflammation IL-1β, IL-6 and TNF-α and amplifies products of oxidative stress 8-iso PGF2α and 8-OHdG in the NG and cNTS. Inhibition of miR-155 signal decreases neuroinflammation and oxidative stress in these pulmonary vagal afferent nerves. Our data suggest the abnormalities in miR-155 pathway of the pulmonary afferent signals at the peripheral and brainstem levels, which is likely to affect respiratory functions as LIRI occurs.

Conflict of interest

The author(s) declare that there is no conflict of interest.

Funding

This research received no specific grant from any funding agency in the public, commercial, or not-for-profit sectors.

References

1. Ailawadi G, Lau CL, Smith PW, et al. Does reperfusion injury still cause significant mortality after lung transplantation? *J Thorac Cardiovasc Surg* 2009; 137: 688–694.
2. Rubenfeld GD, Caldwell E, Peabody E, et al. Incidence and outcomes of acute lung injury. *N Engl J Med* 2005; 353: 1685–1693.
3. Laubach VE and Sharma AK. Mechanisms of lung ischemia-reperfusion injury. *Curr Opin Organ Transplant* 2016; 21: 246–252.
4. Lee LY and Yu J. Sensory nerves in lung and airways. *Comprehen Physiol* 2014; 4: 287–324.
5. Poole DP, Amadesi S, Veldhuis NA, et al. Protease-activated receptor 2 (PAR2) protein and transient receptor potential vanilloid 4 (TRPV4) protein coupling is required for sustained inflammatory signaling. *J Biol Chem* 2013; 288: 5790–5802.
6. Alvarenga EM, Souza LK, Araujo TS, et al. Carvacrol reduces irinotecan-induced intestinal mucositis through inhibition of inflammation and oxidative damage via TRPA1 receptor activation. *Chem Biol Interact* 2016; 260: 129–140.
7. Shi HL, Liu CH, Ding LL, et al. Alterations in serotonin, transient receptor potential channels and protease-activated receptors in rats with irritable bowel syndrome attenuated by Shugan decoction. *World J Gastroenterol* 2015; 21: 4852–4863.
8. Trevisan G, Benemei S, Materazzi S, et al. TRPA1 mediates trigeminal neuropathic pain in mice downstream of monocytes/macrophages and oxidative stress. *Brain* 2016; 139: 1361–1377.
9. Steinberg BE, Silverman HA, Robbiati S, et al. Cytokine-specific neurograms in the sensory vagus nerve. *Bioelectron Med* 2016; 3: 7–17.
10. Undem BJ and Carr MJ. Pharmacology of airway afferent nerve activity. *Respir Res* 2001; 2: 234–244.
11. Bartel DP. MicroRNAs: target recognition and regulatory functions. *Cell* 2009; 136: 215–233.
12. Sayed D and Abdellatif M. MicroRNAs in development and disease. *Physiol Rev* 2011; 91: 827–887.
13. Eacker SM, Dawson TM and Dawson VL. Understanding microRNAs in neurodegeneration. *Nat Rev Neurosci* 2009; 10: 837–841.
14. Farazi TA, Spitzer JI, Morozov P, et al. miRNAs in human cancer. *J Pathol* 2011; 223: 102–115.
15. Han M, Toli J and Abdellatif M. MicroRNAs in the cardiovascular system. *Curr Opin Cardiol* 2011; 26: 181–189.
16. Gambari R, Fabbri E, Borgatti M, et al. Targeting microRNAs involved in human diseases: a novel approach for modification of gene expression and drug development. *Biochem Pharmacol* 2011; 82: 1416–1429.
17. Calame K. MicroRNA-155 function in B Cells. *Immunity* 2007; 27: 825–827.
18. Elton TS, Selemon H, Elton SM, et al. Regulation of the MIR155 host gene in physiological and pathological processes. *Gene* 2013; 532: 1–12.
19. Faraoni I, Antonetti FR, Cardone J, et al. miR-155 gene: a typical multifunctional microRNA. *Biochim Biophys Acta* 2009; 1792: 497–505.
20. O'Connell RM, Rao DS and Baltimore D. microRNA regulation of inflammatory responses. *Annu Rev Immunol* 2012; 30: 295–312.
21. Sonkoly E, Janson P, Majuri ML, et al. MiR-155 is overexpressed in patients with atopic dermatitis and modulates T-cell proliferative responses by targeting cytotoxic T lymphocyte-associated antigen 4. *J Allergy Clin Immunol* 2010; 126: 581–589.e581–520.
22. Moore CS, Rao VT, Durafourt BA, et al. miR-155 as a multiple sclerosis-relevant regulator of myeloid cell polarization. *Ann Neurol* 2013; 74: 709–720.
23. Zhang XH, Qi HX, Xu DS, et al. Expression of proteinase-activated receptor-2 and transient receptor potential A1 in vagal afferent nerve of rat after lung schemia-reperfusion injury. *J Biol Regul Homeostat Agents* 2019; 33: 1405–1413.
24. Karthikeyan A, Patnala R, Jadhav SP, et al. MicroRNAs: key players in microglia and astrocyte mediated inflammation in CNS pathologies. *Curr Med Chem* 2016; 23: 3528–3546.
25. Khoshnam SE, Winlow W and Farzaneh M. The interplay of MicroRNAs in the inflammatory mechanisms following ischemic stroke. *J Neuropathol Exp Neurol* 2017; 76: 548–561.
26. Roitbak T. Silencing a multifunctional microRNA is beneficial for stroke recovery. *Front Mol Neurosci* 2018; 11: 58.
27. Cardoso AL, Guedes JR, Pereira de Almeida L, et al. miR-155 modulates microglia-mediated immune response by down-regulating SOCS-1 and promoting cytokine and nitric oxide production. *Immunology* 2012; 135: 73–88.
28. Yasukawa H, Sasaki A and Yoshimura A. Negative regulation of cytokine signaling pathways. *Ann Rev Immunol* 2000; 18: 143–164.
29. Chinen T, Kobayashi T, Ogata H, et al. Suppressor of cytokine signaling-1 regulates inflammatory bowel disease in which both IFNgamma and IL-4 are involved. *Gastroenterology* 2006; 130: 373–388.
30. Hanada T, Yoshida H, Kato S, et al. Suppressor of cytokine signaling-1 is essential for suppressing dendritic cell activation and systemic autoimmunity. *Immunity* 2003; 19: 437–450.
31. Eisenhardt SU, Weiss JB, Smolka C, et al. MicroRNA-155 aggravates ischemia-reperfusion injury by modulation of inflammatory cell recruitment and the respiratory oxidative burst. *Basic Res Cardiol* 2015; 110: 32.
32. Wen Y, Zhang X, Dong L, et al. Acetylbritannilactone modulates MicroRNA-155-mediated inflammatory response in ischemic cerebral tissues. *Mol Med* 2015; 21: 197–209.
33. Carr MJ and Undem BJ. Bronchopulmonary afferent nerves. *Respirology* 2003; 8: 291–301.
34. Guyenet PG, Stornetta RL and Bayliss DA. Central respiratory chemoreception. *J Comparat Neurol* 2010; 518: 3883–3906.
35. Trankner D, Hahne N, Sugino K, et al. Population of sensory neurons essential for asthmatic hyperreactivity of inflamed airways. *Proc Natl Acad Sci U S A* 2014; 111: 11515–11520.
36. Andersson DA, Gentry C, Moss S, et al. Transient receptor potential A1 is a sensory receptor for multiple products of oxidative stress. *J Neurosci* 2008; 28: 2485–2494.
37. Bandell M, Story GM, Hwang SW, et al. Noxious cold ion channel TRPA1 is activated by pungent compounds and bradykinin. *Neuron* 2004; 41: 849–857.
38. Bautista DM, Movahed P, Hinman A, et al. Pungent products from garlic activate the sensory ion channel TRPA1. *Proc Natl Acad Sci U S A* 2005; 102: 12248–12252.

39. Jordt SE, Bautista DM, Chuang HH, et al. Mustard oils and cannabinoids excite sensory nerve fibres through the TRP channel ANKTM1. *Nature* 2004; 427: 260–265.
40. Sawada Y, Hosokawa H, Matsumura K, et al. Activation of transient receptor potential ankyrin 1 by hydrogen peroxide. *Eur J Neurosci* 2008; 27: 1131–1142.
41. Kwan KY, Allchorne AJ, Vollrath MA, et al. TRPA1 contributes to cold, mechanical, and chemical nociception but is not essential for hair-cell transduction. *Neuron* 2006; 50: 277–289.
42. Story GM, Peier AM, Reeve AJ, et al. ANKTM1, a TRP-like channel expressed in nociceptive neurons, is activated by cold temperatures. *Cell* 2003; 112: 819–829.
43. Lin YJ, Lin RL, Ruan T, et al. A synergistic effect of simultaneous TRPA1 and TRPV1 activations on vagal pulmonary C-fiber afferents. *J Appl Physiol* 2015; 118: 273–281.
44. Bessac BF, Sivula M, von Hehn CA, et al. TRPA1 is a major oxidant sensor in murine airway sensory neurons. *J Clin Invest* 2008; 118: 1899–1910.
45. Trevisani M, Sie, mens J, Materazzi S, et al. 4-Hydroxynonenal, an endogenous aldehyde, causes pain and neurogenic inflammation through activation of the irritant receptor TRPA1. *Proc Natl Acad Sci U S A* 2007; 104: 13519–13524.
46. Kim HJ, Wie J, So I, et al. Menthol modulates pacemaker potentials through TRPA1 channels in cultured interstitial cells of Cajal from murine small intestine. *Cell Physiol Biochem* 2016; 38: 1869–1882.
47. Griton M and Konsman JP. Neural pathways involved in infection-induced inflammation: recent insights and clinical implications. *Clin Autonom Res* 2018; 28: 289–299.